Scientia Horticulturae 257 (2019) 108752

Contents lists available at ScienceDirect

Scientia Horticulturae

journal homepage: www.elsevier.com/locate/scihorti

Effect of cutting on the reactive oxygen species accumulation and energy change in postharvest melon fruit during storage

Zhangfei Wu[a], Mingmei Tu[a], Xingping Yang[b], Jinhua Xu[b], Zhifang Yu[a,*]

[a] College of Food Science and Technology, Nanjing Agricultural University, Nanjing 210095, PR China
[b] Institute of Vegetable Science, Jiangsu Academy of Agricultural Sciences, Jiangsu, 210095, PR China

ARTICLE INFO

Keywords:
Melon fruit
Postharvest
Cutting
Reactive oxygen species
Energy

ABSTRACT

The effect of cutting on the accumulation of reactive oxygen species (ROS) and energy change in melon fruit (cv. Xizhoumi-17, stored at 15 °C) during storage was explored. The key metabolites, enzymes, and genes involved in ROS accumulation and energy metabolism were investigated. Cutting melon fruit changed the respiratory metabolism pathway, increased the respiration rate, and maintained higher activities of H^+-adenosine triphosphatase and Ca^{2+}-adenosine triphosphatase. This led to the large generation of adenosine triphosphate, adenosine diphosphate, NADPH, and NADH in fresh-cut melon fruit. Furthermore, cutting enhanced the NADPH oxidase activity, which induced a higher ROS level and further resulted in higher malondialdehyde content and electrolyte leakage. However, only the activities of peroxidase (POD) and glutathione peroxidase (GPX) were enhanced in fresh-cut melon during the early stage of storage. In addition, lower antioxidant system activity was observed in fresh-cut melon at the late stage of storage. This was indicated by the lower levels of ascorbic acid, glutathione, POD, GPX, ascorbate peroxidase, and glutathione reductase. These lower levels were related to changes of genes related to ROS accumulation and energy metabolism in fresh-cut melon. These findings demonstrate that cut-wounding stress changed the respiratory metabolism pathway in melon fruit and led to a higher energy status, accompanied by increased ROS accumulation.

1. Introduction

The melon (*Cucumis melo* L.) is one of the most popular fruits globally and is the fifth most important fruit worldwide in terms of production (Ortiz-Duarte et al., 2019). Fresh-cut melon is a common product found in stores and supermarkets; however, the quality of fresh-cut melon deteriorates faster due to cutting stress (Gil et al., 2006). Cutting is considered a critical point that divides intact products into smaller cubes or pieces in a fruit and vegetable fresh-cut processing line. The cutting operation inevitably leads to tissue stress due to wounding, thus inducing a number of physiological disorders that need to be minimized to obtain fresh-like quality (Soliva-Fortuny and Martín-Belloso, 2003). The symptoms induced by cutting stress include an increase in respiration rate and ethylene production, dehydration and oxidative browning, loss of flavor and texture, development of off-flavors, membrane breakdown, tissue softening, and decreasing nutrient levels (Hodges and Toivonen, 2008).

Cut-wounding causes the alteration of the carbon metabolism in fruits and vegetables, which induces physiological stress and an increase of the respiration rate (Jacobo-Velázquez et al., 2015). Previous studies suggested that cutting led to an increase of the level of reactive oxygen species (ROS) in carrot (Jacobo-Velázquez et al., 2011), *Zizania latifolia* (Luo et al., 2012), and pitaya (Li et al., 2017a). In addition, wounding accelerates the ripening and senescence of postharvest fruits and vegetables, and ROS in injured fruits may act as signaling molecules in response to cut-wounding stress (Jacobo-Velázquez et al., 2011; Li et al., 2017b), for example, ROS play an important role in the wound-induced activation of both the primary and secondary metabolism in carrot (Jacobo-Velázquez et al., 2015). However, oxidative stress induced overproduction of ROS causes cell death (Iakimova and Woltering, 2018; Reyes et al., 2007), and the necessary balance between ROS generation and antioxidant enzymes activities is closely associated with the ripening and senescence of fruits and vegetables. The release of superoxide radical ($O_2^{\cdot -}$) in postharvest muskmelon fruit was accompanied by enhanced NADPH oxidase (NOX) activity, however, higher activities of superoxide dismutase (SOD) and ascorbate peroxidase (APX) as well as higher contents of ascorbic acid (AsA) and glutathione (GSH) were observed (Ge et al., 2015). This suggested that higher NOX activity can stimulate the production of $O_2^{\cdot -}$ (Shetty et al., 2008) and ROS are then rapidly scavenged by various cellular

* Corresponding author.
E-mail address: yuzhifang@njau.edu.cn (Z. Yu).

https://doi.org/10.1016/j.scienta.2019.108752
Received 30 May 2019; Received in revised form 6 August 2019; Accepted 7 August 2019
Available online 19 August 2019

enzymatic and non-enzymatic mechanisms in postharvest fruits (Ge et al., 2015).

Adenosine triphosphate (ATP) is mostly generated by mitochondrial oxidative phosphorylation and acts as intracellular energy currency. In addition, ATP also acts as a friendly extracellular signaling molecule during postharvest stress and senescence in horticultural crops (Aghdam et al., 2018). Previous studies reported that the energy metabolism is a crucial factor for the modulation of ROS accumulation in postharvest fruits (Aghdam et al., 2018). Lin et al. (2017) reported that exogenous ATP contributed to the higher intracellular supply of ATP and resulted in higher energy charge (EC), higher antioxidant system activity, and a lower ROS level. The energy supply in plant cells plays an important role in the biological metabolism of postharvest fruits and vegetables (Jiang et al., 2007). Furthermore, wounding stress stimulates excessive energy production in pitaya (Li et al., 2018) and exogenous ATP can effectively delay senescence, attenuate stresses, and maintain quality in postharvest fruits (Aghdam et al., 2018); however, exogenous ATP enhanced the $O_2^{\cdot -}$ accumulation in injured *Arabidopsis* leaves (Song et al., 2006).

Earlier studies of ROS level, antioxidant enzymes, and energy status in fresh-cut fruits and vegetables have been conducted (Li et al., 2017a, 2018; Luo et al., 2012); however, the relationship between ROS accumulation and energy status in postharvest fruits and vegetables under wounding stress still remains unclear. Due to the important roles of ROS accumulation and energy metabolism in both ripening and senescence of horticultural crops, the objective of this work was to investigate the effect of cutting on the ROS accumulation and energy metabolism in postharvest melon during storage at 15 °C. Furthermore, the relationship between ROS accumulation and energy change in melon subjected to cut-wounding stress was explored.

2. Materials and methods

2.1. Fruit material and experimental design

Melon fruits "Xizhoumi-17" (*Cucumis melo* L. var. *reticulatus* Nand.) at the commercially mature stage were picked on October 14, 2017, in Xinghua, Jiangsu Province, China, were transported to the laboratory at Nanjing Agricultural University immediately after harvest, and were then stored at 21 °C for 24 h. Fruits with uniform size, shape, and without mechanical damage were selected and divided into two groups. The first group was used as whole melon samples, and the second group was used for fresh-cutting samples. For the fresh-cut samples, melons were manually peeled, cut into 2.0 × 2.0 × 2.0 cm cubes, and then packaged into rigid plastic boxes (17.2 × 12.0 × 6.8 cm, 120 ± 5 g fresh-cut cubes per box).

Whole melon fruit were stored at 15 °C (WF group) and sampled on days 0, 2, 4, 8, and 12, while fresh-cut melon cubes stored at 15 °C (FC group) were sampled on days 0, 1, 2, 3, and 4. At each time point, 10 fruits per sample were taken for analysis, and all samples were conducted in triplicate. The pulp from the center of the sampled melons was immediately frozen in liquid nitrogen and all frozen samples were stored at −80 °C for further analysis.

2.2. Determination of respiration rate

At each time point, four melon fruits of the WF group were randomly chosen from each biological repetition and enclosed in 25 L plastic jars at 25 °C for 1 h. Fresh-cut cubes (110 ± 10 g) were enclosed in 1 L plastic jars at 25 °C for 1 h. After storage for 1 h, the relative content of CO_2 (compared to air) in the plastic jars was determined by a CO_2 gas analyzer (Check Mate 3, Dansensor, Denmark). The respiration rate was expressed as mg h^{-1} kg^{-1} of CO_2 based on fresh weight.

2.3. Determination of $O_2^{\cdot -}$ and hydrogen peroxide (H_2O_2) contents

Each fresh sample (3.0 g) was homogenized with 5 mL of 65 mM sodium phosphate buffer (pH 7.8) and then centrifuged at 10,000 × g for 20 min at 4 °C. The supernatant was used to determine the $O_2^{\cdot -}$ production rate according to the method of Chen et al. (2017). The $O_2^{\cdot -}$ content was calculated using $NaNO_2$ as standard and was expressed as mmol kg^{-1} based on fresh weight.

Each fresh sample (3.0 g) was homogenized with 5 mL ice-cold acetone and then centrifuged at 8000 × *g*at 4 °C for 20 min. The supernatant was used for the determination of H_2O_2 using the method of Chen et al. (2017). The H_2O_2 content was expressed as μmol kg^{-1} based on fresh weight.

2.4. Determination of electrolyte leakage (EL) and malondialdehyde (MDA) content

EL was measured with the method of Chen et al. (2017). Twenty disks (5 mm diameter × 1 mm thickness) of flesh tissue of 10 melon fruits were immersed in 40 mL of deionized water in glass vials for 1 h at 25 °C. The conductivity was assayed immediately (C_1) and the disks were then boiled for 5 min to measure the resulting conductivity (C_2). The relative electrolyte leakage was determined as C_1 / C_2 × 100.

To measure the MDA content, each fresh sample (3.0 g) was homogenized in 5 ml of 50 mM sodium phosphate buffer (pH 7.8). The MDA content was measured following the method of Chen et al. (2017) and expressed as μmol kg^{-1} based on fresh weight.

2.5. Determination of AsA and GSH contents

To measure the AsA content, frozen melon tissue (20.0 g) of each sample was ground in liquid nitrogen. The obtained frozen melon powder (2.0 g) was then homogenized with 6 ml of 0.1% oxalic acid (v/v) for 10 min at 4 °C, followed by centrifugation at 10,000 × g for 20 min at 4 °C. The supernatant was filtered by a 0.45-μm filter. 20 μL of the filtrate was injected into the high performance liquid chromatography (HPLC) system (Model LC-20A, GL Sciences, Japan) equipped with a ZORBAX SB-Aq C18 column (5 μm, 4.6 × 250 mm, Shimadzu, Japan) to measure the AsA content according to the method used by Xu et al. (2008) with minor modifications. Oxalic acid solution (0.1%, v/v) was used as mobile phase at a flow rate of 1.0 mL min^{-1} at 25 °C and the AsA content was measured at a wavelength of 243 nm with a photodiode array detector.

The GSH content was assayed according to the method of Wang et al. (2018). Frozen melon powder (2.0 g) was homogenized with 4 ml of chilled trichloroacetic acid (50 g L^{-1}) containing 5.0 mM ethylenediaminetetraacetic acid (EDTA) and the mixture was centrifuged at 10,000 × *g*for 20 min at 4 °C. The reaction mixture contained 1.0 ml of supernatant, 1.0 ml of 100 mM sodium phosphate buff (pH 7.8), and 0.5 ml of 4 mM 5,5′-dithiobis (2-nitrobenzoic acid). The AsA and GSH contents were quantified according to standard curves and were expressed as mg kg^{-1} and g kg^{-1}, respectively, based on fresh weight.

2.6. Determination of NAD(H) and NADP(H) contents

Frozen melon powder (0.5 g) was homogenized in 5 ml of 0.1 M HCl for NAD and NADP determination or in 5 ml of 0.1 M NaOH for NADH and NADPH determination. The homogenates were heated in a boiling water bath for 5 min and then cooled in an ice bath, followed by centrifugation at 10,000 × *g*for 10 min at 4 °C. The supernatants were neutralized with 0.1 M NaOH or HCl and then centrifuged at 10,000 × *g*for 10 min at 4 °C. The re-supernatants were collected for the determination of NAD(H) and NADP(H) using the method of Gibon and Larher (1997) and the results were expressed as mmol kg^{-1} based on fresh weight.

2.7. Analysis of ATP, adenosine diphosphate (ADP), adenosine monophosphate (AMP), and EC

Frozen melon powder (2.0 g) was homogenized with 4 mL of 600 mM perchloric acid, followed by centrifugation at 8000 × *g*for 10 min at 4 °C. 4 mL of the collected supernatant was adjusted to pH 6.5–6.8 by KOH (1 M), followed by dilution to 6 mL with ultrapure water, and filtering by a 0.45-μm filter. 20 μL of the filtrate was injected into a HPLC system (Model LC-20A, GL Sciences, Japan) equipped with a ZORBAX SB-Aq C18 column (5 μm, 4.6 × 250 mm, Shimadzu, Japan) to analyze the contents of ATP, ADP, and AMP according to the method of Palma et al. (2015) with slight modifications. Chromatograms were detected at 254 nm by a photodiode array detector. Methanol (A) and 100 mM potassium phosphate buffer (B, pH 7.0) were used as mobile phases. Elution was conducted by a linear gradient program set to 0/0, 7/20, 9/25, 10/0, and 15/0 (min/% solvent A) at a flow rate of 1.0 mL min^{-1} at 25 °C. ATP, ADP, and AMP contents were calculated via standard curves with standard samples and expressed as mg kg^{-1} based on fresh weight. EC was calculated using the following formula: EC = (ATP + 1/2 ADP) / (ATP + ADP + AMP).

2.8. Analysis of enzyme activities involved in ROS and energy metabolism

To measure the NOX activity, frozen melon powder (2.0 g) was homogenized with 5 mL of 25 mM MES buffer (pH 7.8) containing polyvinylpolypyrrolidone (0.9%, m/v), 0.25 M sucrose, 1 mM phenylmethanesulfonyl fluoride, 3 mM EDTA, and 5 mM dithiothreitol (DTT). The homogenate was placed in an ice bath for 10 min, followed by centrifugation at 12,000 × g for 30 min at 4 °C. The pellet was dissolved in 1 mL 5 mM MES buffer (pH 7.8) containing 0.25 M sucrose, 1 mM phenylmethanesulfonyl fluoride, 5 mM DTT, and 5 mM KCl. The suspension was used as crude enzyme extract. The NOX activity was measured following the method reported by Sagi and Fluhr (2001). 1.2 mL of the reaction mixture containing 50 mM Tris-HCl buffer (pH 7.5), 50 mM 2,3-bis(2-methoxy-4-nitro-5-sulfophenyl)-5-(phenylamino) carbonyl-2H-tetrazolium hydroxide (XTT), and 100 μM EDTA. The reaction was initiated by adding 0.2 mL crude enzyme extract and 0.1 mL 1 mM NADPH. One unit of NOX activity was calculated as the amount of enzyme that reduced 1 μmol XTT per min at A_{470} and was expressed as U mg^{-1} based on protein content.

SOD activity was measured according to the method of Luo et al. (2012). One unit of SOD activity was defined as the quantity of enzyme that caused 50% inhibition of nitro blue tetrazolium per min at A_{560} and was expressed as U mg^{-1} based on protein content.

The APX activity was assayed using the method of Wang et al. (2018). One unit of APX activity was defined as the amount of enzyme that oxidized 1 μmol of ascorbate per min at A_{290} and was expressed as U mg^{-1} based on protein content.

Peroxidase (POD) activity was determined according to the method of Luo et al. (2012). One unit of POD activity was calculated as the amount of enzyme that oxidized 1 μmol guaiacol per min at A_{470} and was expressed as U mg^{-1} based on protein content.

Glutathione reductase (GR) and glutathione peroxidase (GPX) activities were determined according to Cocetta et al. (2014) and Huan et al. (2016), respectively. One unit of GR or GPX activity was calculated as the amount of enzyme that oxidized 1 μmol NADPH per min at A_{340} and was expressed as U mg^{-1} based on protein content.

Phosphohexose isomerase (PGI) activity was measured using the method of Li et al. (2016). One unit of PGI activity was calculated as the amount of enzyme that produced 1 μmol fructose-6-phosphate per h and was expressed as U mg^{-1} based on protein content.

The total activity of both glucose-6-phosphate dehydrogenase (G-6-PDH) and 6-phosphogluconate dehydrogenase (6-PGDH) was determined according to the method of Guo et al. (2013). One unit of total activity of G-6-PDH and 6-PGDH was calculated as the amount of enzyme that produced 1 μmol NADPH per min at A_{340} and was expressed as U mg^{-1} based on protein content.

The crude mitochondria of melon tissue were prepared according to the method of Wang et al. (2015). The crude mitochondria extract was obtained for the analysis of enzymes related to the energy metabolism.

The activities of succinate dehydrogenase (SDH) and cytochrome c oxidase (CCO) were assayed according to the method of Acevedo et al. (2013) and Errede et al. (1978), respectively, with modifications. 1.2 mL of the reaction mixture, containing 50 mM potassium phosphate buffer (pH 7.8), 0.08 mM dichlorophenol indophenol sodium, and 100 mM sodium succinate, was incubated at 30 °C for 5 min. 0.2 mL of crude mitochondria extract and 0.1 mL of phenazine methosulfate were added to the reaction mixture and the change of absorbance at A_{600} was measured immediately. One unit of SDH activity was calculated as the increase of 0.01 of absorbance at A_{600} per min and was expressed as U mg^{-1} based on protein content.

To measure the CCO activity, 2.8 mL of the reaction mixture, which contained 50 mM potassium phosphate buffer (pH 7.5), 20 mM dimethyl phenylenediamine, and 0.3 mM cytochrome c, was incubated at 37 °C for 2 min. 0.2 mL of crude mitochondria extract was added to the reaction mixture and the change of absorbance at A_{510} was measured immediately. One unit of CCO activity was defined as the change of 0.01 of absorbance at A_{510} per min and was expressed as U mg^{-1} based on protein content.

The activities of H^+-adenosine triphosphatase (H^+-ATPase) and Ca^{2+}-adenosine triphosphatase (Ca^{2+}-ATPase) were assayed using the method of Li et al. (2018). One unit of H^+-ATPase or Ca^{2+}-ATPase activity was calculated as the amount of enzyme that produced 1 nmol of phosphorus per min and was expressed as U mg^{-1} based on protein content. All of the above protein content of crude enzyme extract were estimated according to the method of Bradford (1976), using bovine serum albumin as standard.

2.9. RNA isolation and mRNA expression analysis

Genes involved in ROS accumulation and energy metabolism were identified from the CuGenDB (http://cucurbitgenomics.org/) and had been analyzed by transcriptome (data not shown). Total RNA was extracted from each sample of melon tissue using the RNAprep Pure Plant Kit (DP441, TIANGEN, China) according to the manufacturer's instructions. First-strand cDNA was synthesized using the PrimeScript™ RT Master Mix (RR036A, TaKaRa, Japan) following the manufacturer's instructions. Gene-specific primers (Table S1) were designed with Primer 5.0 software. Real-time quantitative reverse transcription PCR (qRT-PCR) was used to analyze the gene expression with Applied Biosystems 7500 Fast Real-Time PCR System (Applied Biosystems, USA) using the SYBR® Premix Ex Taq™ (RR420A, TaKaRa, Japan) in a 20-μL system. The qRT-PCR was performed using a thermo cycling that was set with an initial denaturation at 95 °C for 30 s, followed by 40 cycles of 95 °C for 3 s and 60 °C for 1 min. Relative gene expression was calculated using the "Comparative $2^{-\Delta\Delta CT}$" method with *β-actin* as the reference gene, and the gene expression of fruit at day 0 was set to 1.

2.10. Statistical analysis

Data are expressed as means ± standard error (SE) of three replicates and analyzed by one-way analysis of variance (ANOVA) using SPSS 17.0 (SPSS Inc., Chicago, IL, USA). The mean separations were analyzed using Duncan's multiple range test and differences were considered to be statistically significant at $p < 0.05$.

3. Results

3.1. Respiration rate

Fig. 1A shows that the respiration rate of both whole and fresh-cut melon decreased during storage at 15 °C. The respiration rate of fresh-

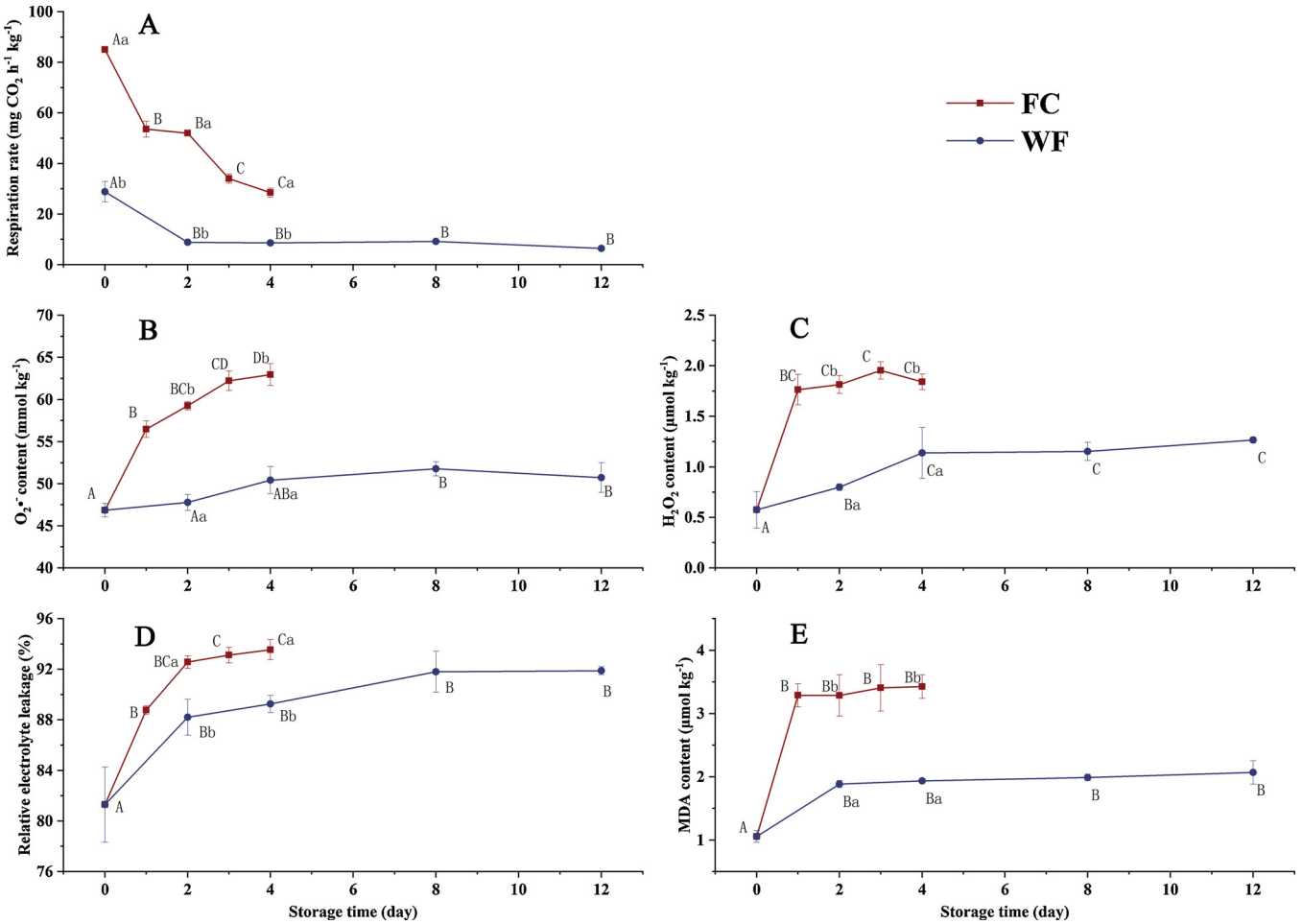

Fig. 1. Effect of cutting on the (A) respiration rate, (B) superoxide radical ($O_2^{\cdot -}$) content, (C) hydrogen peroxide (H_2O_2) content, (D) relative electrolyte leakage (EL) and (E) malondialdehyde (MDA) content in melon fruit during storage at 15 °C. FC: fresh-cut melon fruit; WF: whole melon fruit. The values are expressed as means ± SE of three replicates. Values with different letters indicate statistically significant differences ($p < 0.05$). Lowercase letters represent significant differences between fresh-cut melon and whole fruit at the same time point, capital letters represent significant difference among storage time factors.

cut melon was significantly higher than that of whole fruit during the storage period and showed a 2.9-fold increase in comparison with whole fruit at day 0. This sudden increase of respiration rate may result from accelerated metabolism caused by cut-wounding (Amaro et al., 2012). These results indicate that cutting stimulated the respiration rate.

3.2. Contents of $O_2^{\cdot -}$ and H_{2O_2}

As shown in Fig. 1B and C, $O_2^{\cdot -}$ and H_2O_2 contents increased slightly with storage time in whole fruit, while $O_2^{\cdot -}$ and H_2O_2 contents in fresh-cut melon increased rapidly immediately after cutting and maintained at higher level until the end of storage. These results suggest that cutting induced higher oxidative stress in melon as indicated by the higher contents of $O_2^{\cdot -}$ and H_2O_2, which accelerated the cell death in fresh-cut melon.

3.3. Relative EL and MDA content

The relative EL showed a gradual increase in both groups and was consistently higher in fresh-cut melon (Fig. 1D). The MDA content of whole fruit increased greatly immediately after harvest and then remained stable during storage. However, the MDA content of fresh-cut melon showed a sharp increase at day 1 and then remained almost twice as high as that in whole fruit from day 1 to 4 (Fig. 1E). These data were consistent with the change of $O_2^{\cdot -}$ and H_2O_2 as shown in Fig. 1B and C. EL and MDA are indicators that are used to indirectly assess cell membrane integrity and reflect the intensity of oxidative stress in postharvest fruits and vegetables (Huan et al., 2016; Sharom et al., 1994). These data show that cutting induced higher intensity of oxidative stress and severely destroyed the cell membrane integrity as indicated by the higher levels of relative EL and MDA.

3.4. Contents of AsA and GSH

The content of AsA decreased in both groups over the storage period. The AsA content in fresh-cut melon decreased rapidly and displayed a remarkably lower level compared with whole fruit during the storage (Fig. 2A). The GSH content in whole fruit remained stable during the initial two days, which was followed by a sudden decline at day 4 and decreased slowly during the later storage period. However, the GSH content in fresh-cut melon exhibited a decreasing trend during storage and also showed noticeably lower level, similar to AsA (Fig. 2B). These findings suggest that cutting accelerated the decline of AsA and GSH in melon during storage, which may be attributed to the oxidation and elimination of AsA and GSH around the injured site (Li et al., 2018).

3.5. NADP(H) and NAD(H) contents

As shown in Fig. 3A, the NADPH content of whole fruit increased after two days of storage, which was followed by a slight decrease.

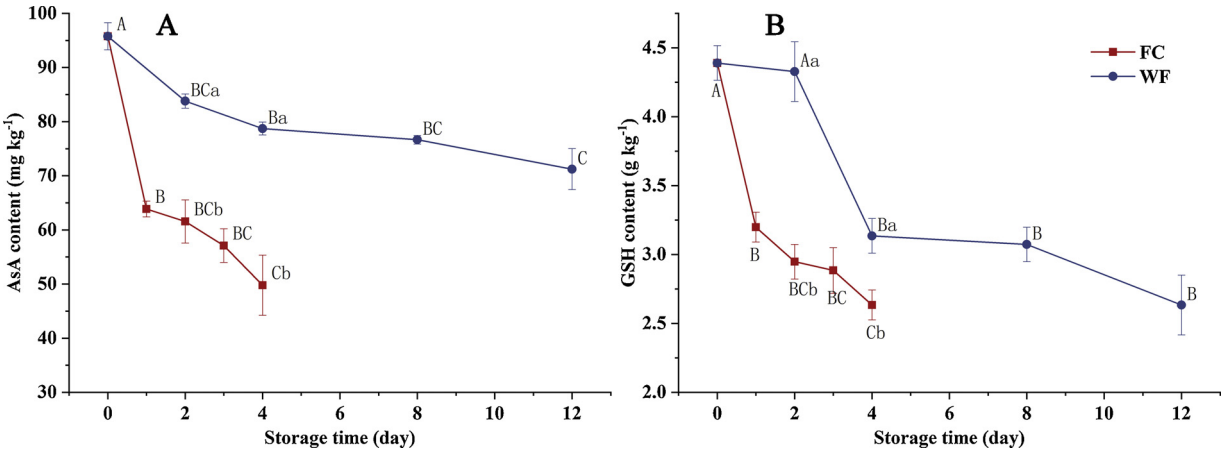

Fig. 2. Effect of cutting on the contents of (A) ascorbic acid (AsA) and (B) glutathione (GSH) in melon fruit during storage at 15 °C. The values are expressed as means ± SE of three replicates. Values with different letters indicate statistically significant differences ($p < 0.05$). Lowercase letters represent significant differences between fresh-cut melon and whole fruit at the same time point, capital letters represent significant difference among storage time factors.

However, in fresh-cut melon, this greatly increased at day 1, decreased at the later stage of storage, and maintained a higher level during storage in comparison with whole fruit. Fig. 3B shows that the NADP content in whole fruit decreased slightly during the storage period, while the NADP content in fresh-cut melon decreased at day 1 and then retained a lower level compared with whole fruit. Compared to the fact that the NADH content in whole fruit showed a decreasing trend with storage duration, the NADH content in fresh-cut melon displayed an initial increase, a significant decrease afterward, and maintained a higher level only at the early stage of storage (Fig. 3C). The content of NAD in whole fruit showed a similar changing pattern than NADP, but a slight decrease in the content of NAD of fresh-cut melon was observed at day 1 followed by a sharply decrease during storage (Fig. 3D). These data indicate that cutting induced an increase of the NAD(P)H content and a decreased NAD(P) content, which may be related to higher respiration rate.

3.6. Contents of ATP, ADP, and AMP and EC level

ATP and ADP contents of whole fruit decreased sharply just after

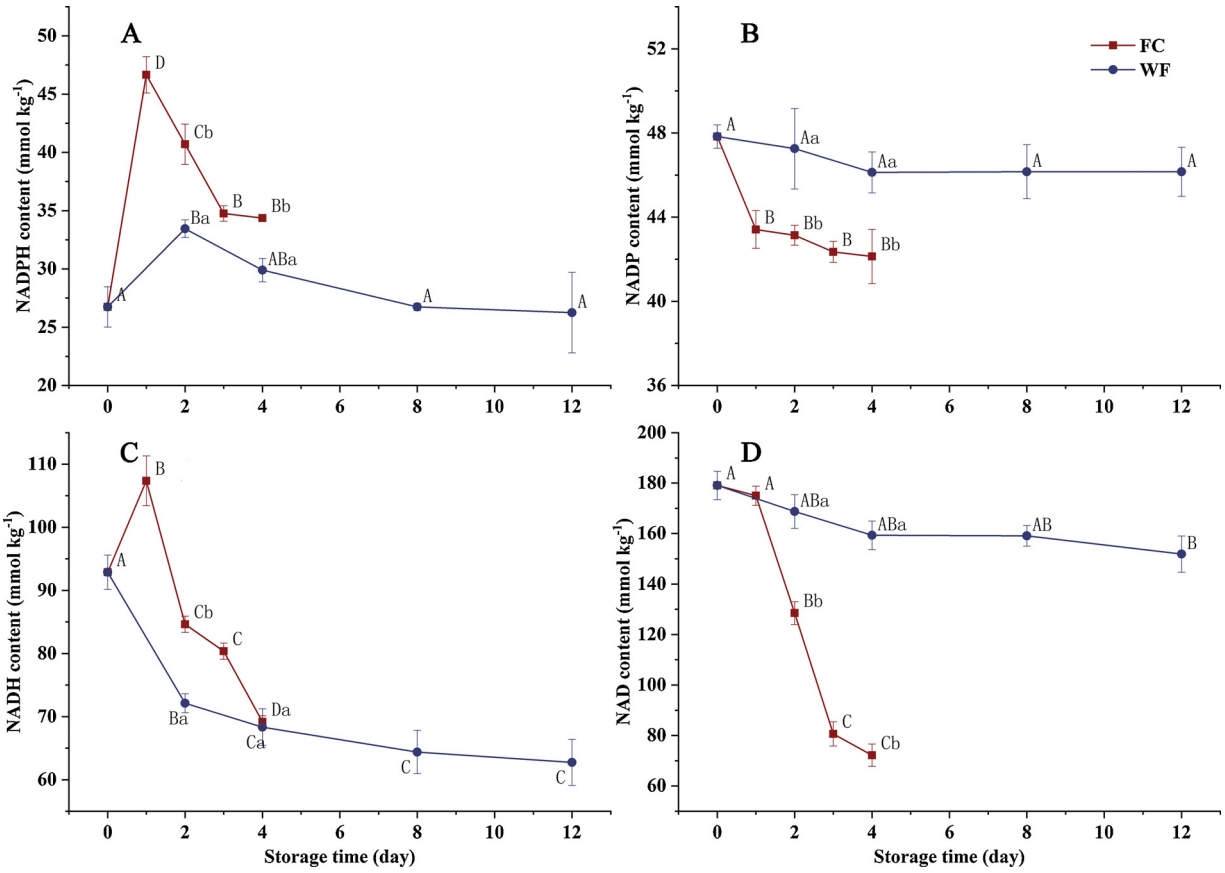

Fig. 3. Effect of cutting on the contents of (A) NADPH, (B) NADP, (C) NADH and (D) NAD in melon fruit during storage at 15 °C. The values are expressed as means ± SE of three replicates. Values with different letters indicate statistically significant differences ($p < 0.05$). Lowercase letters represent significant differences between fresh-cut melon and whole fruit at the same time point, capital letters represent significant difference among storage time factors.

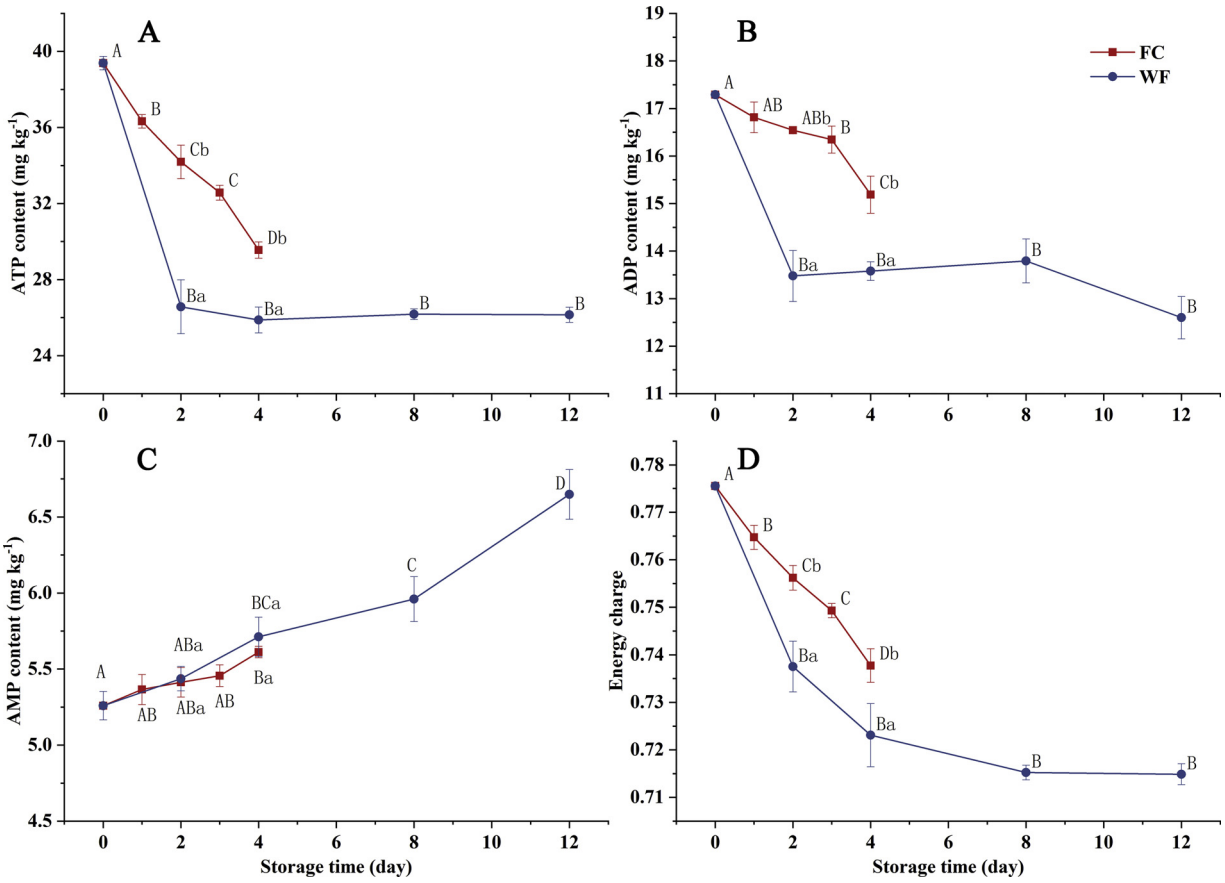

Fig. 4. Effect of cutting on ATP (A), ADP (B) and AMP (C) contents and energy charge (D) in melon fruit during storage at 15 °C. The values are expressed as means ± SE of three replicates. Values with different letters indicate statistically significant differences ($p < 0.05$). Lowercase letters represent significant differences between fresh-cut melon and whole fruit at the same time point, capital letters represent significant difference among storage time factors.

harvest for up to two days, after which, they remained stable at the later storage stage. However, in fresh-cut melon, these contents decreased with storage time and exhibited higher levels until the end of storage compared with whole fruit (Fig. 4A, B). Moreover, the AMP content increased consistently with storage duration in both groups and no significant difference was found between both groups (Fig. 4C). The EC level of both whole and fresh-cut melon during storage decreased sharply with significantly higher values for fresh-cut melon (Fig. 4D). It seems that cutting can stimulate biological reactions and produce more energy (ATP and ADP), thus resulting in higher EC level.

3.7. Activities and gene expression patterns of enzymes related to the ROS metabolism

NOX activity of whole fruit changed slightly during the storage period, while that of fresh-cut melon increased sharply after cutting and maintained a higher level during storage (Fig. 5A). Expression of *CmNOX* in fresh-cut melon was significantly higher than in whole fruit, which was consistent with the observed change in NOX activity (Fig. 5G). These results suggest that cutting could stimulate the expression of *CmNOX*, thus leading to a higher NOX activity in fresh-cut melon.

The changes of antioxidant enzymes activities and gene expression are shown in Fig. 5. The SOD activity in whole and fresh-cut melon decreased sharply early and then remained steady. No significant differences were found between both groups (Fig. 5B). Unlike SOD, POD activity in both groups clearly increased first and then significantly decreased; however, POD activity of fresh-cut melon was higher than that of whole fruit during the early stage of storage and remained lower thereafter (Fig. 5C). The activities of APX and GR in fresh-cut melon were significantly decreased during storage compared with whole fruit (Fig. 5D and E). Moreover, Fig. 5F shows that the GPX activity had a gradual decrease in both groups and was only elevated in fresh-cut melon at day 2 in comparison with whole fruit. Compared with whole fruit, the expressions of *CmSOD*, *CmAPX*, and *CmGR* in fresh-cut melon were decreased during the storage period (Fig. 5H, J and K); however, the expressions of *CmPOD* and *CmGPX* in fresh-cut melon were stimulated after cutting and maintained a higher level throughout the entire storage period (Fig. 5I and L).

These results indicate that cutting enhanced the expressions of *CmPOD* and *CmGPX* and inhibited the expressions of *CmAPX* and *CmGR*, thus resulting in higher activities of POD and GPX and lower activities of APX and GR in fresh-cut melon. It is interesting that the POD activity of fresh-cut melon was higher at the early stage of storage and then lowered when *CmPOD* expression still remained higher at the late stage of storage. This indicates that the lower POD activity in fresh-cut melon at day 4 may be the result of quality deterioration. However, SOD activity showed no obvious change between both groups when the expression of *CmSOD* was lower in fresh-cut melon. The relationship of the SOD activity between whole and fresh-cut melon was inconsistent with the relationship of *CmSOD* expression in both groups, which may be due to the post-transcriptional regulation of SOD.

3.8. Activities and gene expression patterns of enzymes related to the energy metabolism

In comparison with the increasing PGI activity in whole fruit during the storage period, that in fresh-cut melon was enhanced at the early stage of storage and was decreased at the end of storage (Fig. 6A). Unlike PGI, SDH activity of whole fruit declined after two days of

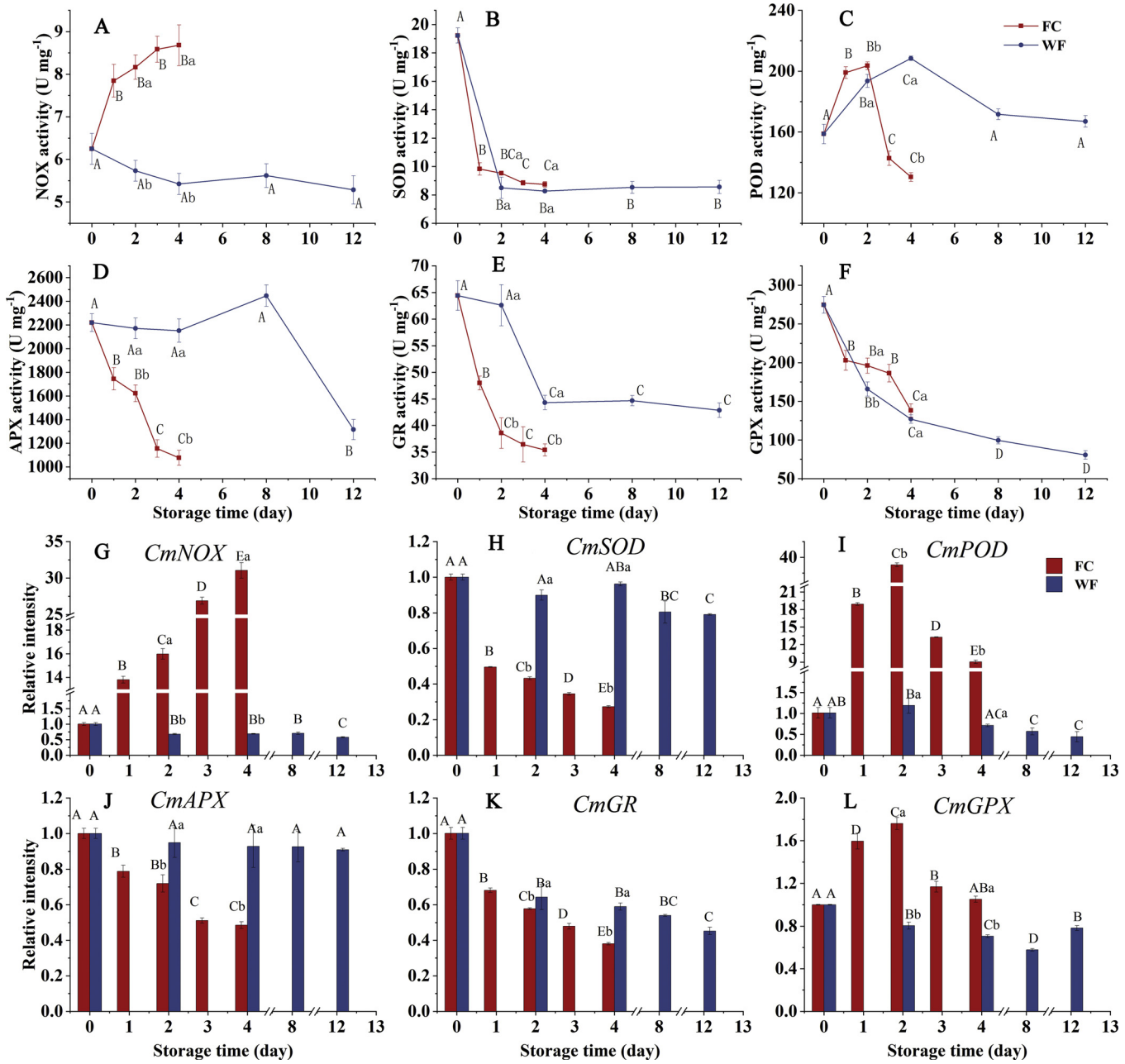

Fig. 5. Effect of cutting on the activities of (A) NADPH oxidase (NOX), (B) superoxide dismutase (SOD), (C) peroxidase (POD), (D) ascorbate peroxidase (APX), (E) glutathione reductase (GR) and (F) glutathione peroxidase (GPX) and relative expression levels of (G) *CmNOX*, (H) *CmSOD*, (I) *CmPOD*, (*J*) *CmAPX*, (K) *CmGR* and (L) *CmGPX* in melon fruit during storage at 15 °C. The values are expressed as means ± SE of three replicates. Values with different letters indicate statistically significant differences ($p < 0.05$). Lowercase letters represent significant differences between fresh-cut melon and whole fruit at the same time point, capital letters represent significant difference among storage time factors.

storage and then remained stable, and the total activity of G-6-PDH and 6-PGDH and the CCO activity in whole fruit continued to decrease during storage. The activities of SDH and CCO and the total activity of G-6-PDH and 6-PGDH in fresh-cut melon decreased with storage time. However, compared with whole fruit, fresh-cut melon had higher activity of SDH, higher total activity of G-6-PDH and 6-PGDH, and lower CCO activity (Fig. 6B–D). As shown in Fig. 6G, the expression of *CmPGI* in both groups showed similar patterns compared with PGI activity, and the *CmPGI* expression in fresh-cut melon was only up-regulated at the early stage of storage in comparison with whole fruit. The expressions of *CmSDH*, *CmG6PDH*, and *Cm6PGDH* in fresh-cut melon increased compared to whole fruit and peaked at days 2, 1, and 2, respectively (Fig. 6H–J). In addition, the expression of *CmCCO* in both groups was consistent with the observed change in CCO activity, and was also lower in fresh-cut melon (Fig. 6K).

PGI, SDH, and CCO are key enzymes in embden-meyerhof-parnas (EMP) pathway, the tricarboxylic acid cycle (TCA) pathway, and cytochrome (CCP) pathway, respectively. G-6-PDH and 6-PGDH are critical regulatory enzymes of the pentose phosphate (PPP) pathway, which directly affects the activation of the PPP pathway. These data suggest that cutting can result in higher levels of EMP, TCA, and PPP in melon, which may be regulated by *CmPGI*, *CmSDH*, *CmG6PDH*, and *Cm6PGDH*, respectively. However, the level of EMP pathway in fresh-cut melon was significantly lower at the end of storage compared with whole fruit. On the contrary, cutting of melon led to a lower level of CCP pathway as indicated by lower CCO activity, which may be caused

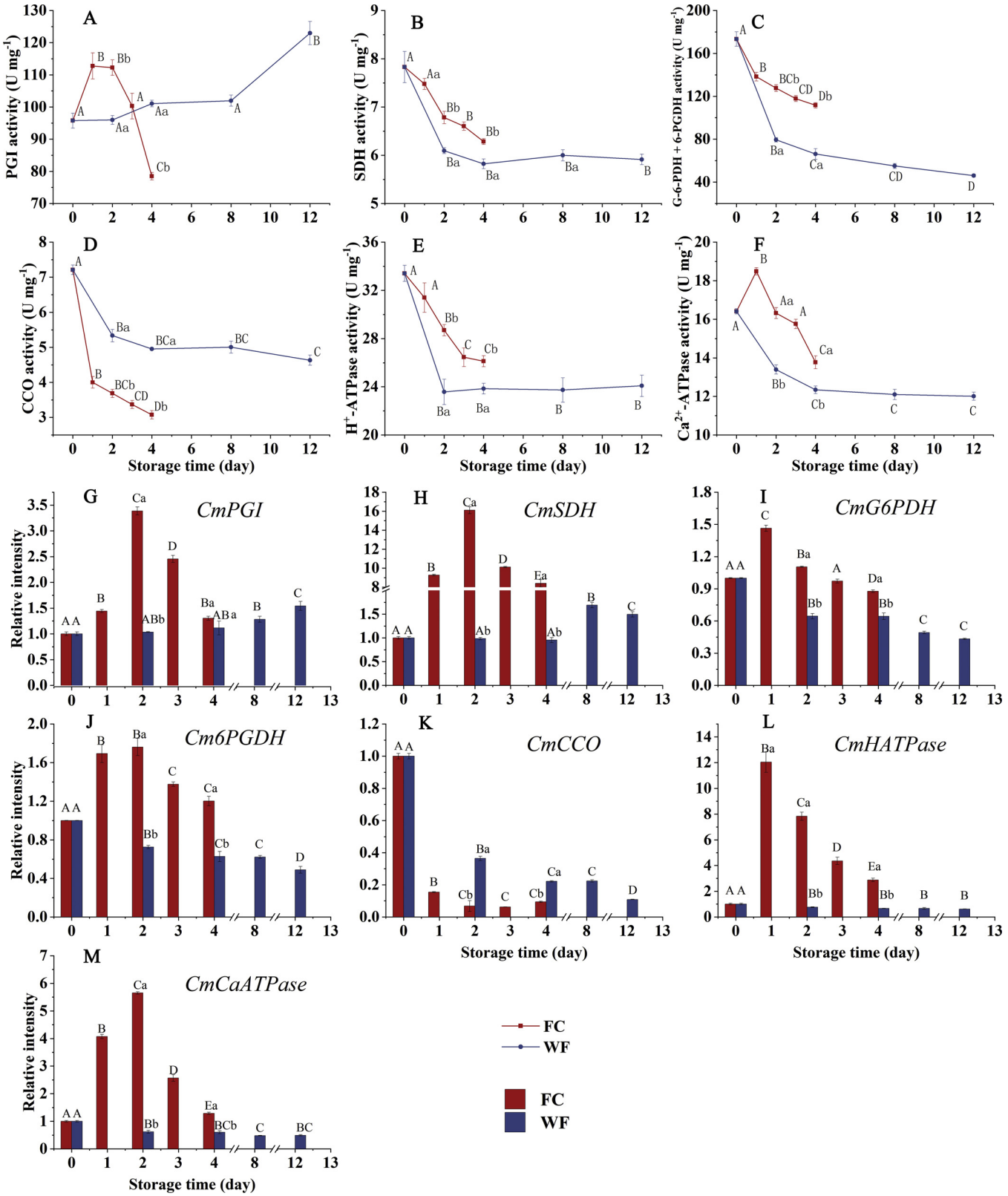

Fig. 6. Effect of cutting on the activities of (A) phosphohexose isomerase (PGI), (B) succinate dehydrogenase (SDH), (C) glucose-6-phosphate dehydrogenase and 6-phosphogluconate dehydrogenase (G-6-PDH + 6-PGDH), (D) cytochrome c oxidase (CCO), (E) H^+-adenosine triphosphatase (H^+-ATPase) and (F) Ca^{2+}-adenosine triphosphatase (Ca^{2+}-ATPase) and relative expression levels of (G) *CmPGI*, (H) *CmSDH*, (I) *CmG6PDH*, (J) *Cm6PGDH*, (K) *CmCCO*, (L) *CmHATPase* and (M) *CmCaATPase* in melon fruit during storage at 15 °C. The values are expressed as means ± SE of three replicates. Values with different letters indicate statistically significant differences ($p < 0.05$). Lowercase letters represent significant differences between fresh-cut melon and whole fruit at the same time point, capital letters represent significant difference among storage time factors.

by lower expression of *CmCCO* in fresh-cut melon.

The activities of H^+-ATPase and Ca^{2+}-ATPase in whole fruit decreased at the early stage of storage and changed slightly afterward. Moreover, H^+-ATPase and Ca^{2+}-ATPase activities in fresh-cut melon also showed a decreasing trend and were higher than that of whole fruit, although the Ca^{2+}-ATPase activity in fresh-cut melon was transiently increased at the earlier stage of storage (Fig. 6E and F). Furthermore, the expressions of *CmHATPase* and *CmCaATPase* in fresh-cut melon were stimulated after cutting, peaked at days 1 and 2, respectively, and maintained a higher level during the storage compared with whole fruit (Fig. 6L and M). These results indicate that higher H^+-ATPase and Ca^{2+} ATPase activities were observed in fresh-cut melon, which may result from the higher expressions of *CmHATPase* and *CmCaATPase*. These changes were consistent with changes of ATP, ADP, and EC level, and a large amount of energy may be produced in fresh-cut melon.

4. Discussion

Although numerous previous studies have reported that cut-wounding enhanced ROS level in postharvest fruits and vegetables (Jacobo-Velázquez et al., 2011; Li et al., 2017a; Luo et al., 2012), the research about the relationship between ROS accumulation and energy change in response to cut-wounding stress in postharvest fruits and vegetables is scarce. This study explored the energy change of whole and fresh-cut melon fruit in relation to ROS accumulation. The data show that melon that was subjected to cut-wounding stress showed a higher respiration rate. This further led to a higher energy status as indicated by higher contents of ATP and ADP as well as higher EC level, which was accompanied by higher ROS accumulation.

EL and MDA content as well as ROS level are indicators of membrane integrity and oxidative stress in fruits (Huan et al., 2016; Sharom et al., 1994). The present study shows that cutting of melon increased the respiration rate and caused higher ROS level, which further induced higher MDA content and EL in fresh-cut melon compared to whole fruit (Fig. 1), these results are consistent with a previous report about fresh-cut *Zizania latifolia* (Luo et al., 2012). This finding suggests that cutting induced higher oxidative stress and membrane damage in melon during storage, which may accelerate the quality deterioration of fresh-cut melon.

NOX is one of the sources of ROS in the oxidative burst and can use NADPH as an electron donor to catalyze the conversion of O_2 to $O_2^{\cdot -}$ (Song et al., 2006), which was also demonstrated by the higher *CmNOX* expression and the higher NOX activity when the $O_2^{\cdot -}$ content was higher in fresh-cut melon in this experiment. O_2 is catalyzed to $O_2^{\cdot -}$ by NOX in plant tissue, and then SOD scavenge $O_2^{\cdot -}$ into H_2O_2, H_2O_2 can further be converted into H_2O by catalase, POD, GPX, and APX (Huan et al., 2016; Wang et al., 2018). The results of the present study suggest that cutting only enhanced the activities of POD and GPX of melon at the early stage of storage (Fig. 5), which is inconsistent with the results of previous studies on pitaya and *Zizania latifolia* (Li et al., 2017b; Luo et al., 2012). The difference may be related to the type of fruit or vegetable tissue, cutting styles, or storage conditions (Reyes et al., 2007). Moreover, lower antioxidant system activity was found in fresh-cut melon at the late stage of storage, while the ROS level still remained high. The POD and GPX activities of fresh-cut melon may be stimulated by the higher ROS level (Luo et al., 2012), the increased activities of POD and GPX in fresh-cut melon contributed to the elimination of excess H_2O_2. However, the activity of POD was decreased when *CmPOD* expression still retained a higher level at the late stage of storage; this further resulted in higher content of H_2O_2 in fresh-cut melon. AsA and GSH act as antioxidants of non-enzymatic mechanisms in plants and react with ROS directly (Wang et al., 2018). This may lead to a decrease of AsA and GSH in fresh-cut melon, which further led to lower APX and GR activities and higher GPX activity where the conversion of GSH to oxidized glutathione may be achieved (Figs. 2A, 5F and 5G).

From above all, compared with whole fruit, cutting induced higher NOX activity in fresh-cut melon, which increased the production of ROS and further led to higher MDA content, where only the activities of POD and GPX were enhanced at the early stage of storage. This may be a significant factor for the quality deterioration in fresh-cut melon.

Cutting caused a rapid increase of the respiratory rate in melon (Fig. 1A). Fig. 6A shows that the level of EMP pathway of fresh-cut melon was enhanced after cutting and was lower at the end of storage, as compared to whole fruit. The lower level of the EMP pathway at the end of storage may be related to the observed decrease of sugar content (data not shown). The EMP pathway oxidizes glucose to pyruvate under the production of ATP, which is subsequently followed by TCA and CCP. Unlike the EMP pathway, the TCA and PPP pathways of fresh-cut melon retained higher levels throughout the entire storage period (Fig. 6B and C). The TCA and PPP pathways can supply intermediate reaction products, which participate in the secondary metabolism. The enhancement of the PPP pathway can increase the capability of plants to endure abiotic stress (Ślaski et al., 1996), indicating that fresh-cut melon could improve its ability to defend the cut-wounding stress. A similar result was also reported for the postharvest storage of broccoli (Li et al., 2016). However, the CCP pathway of fresh-cut melon displayed lower level as indicated by lower CCO activity (Fig. 6D), this result is likely related to higher ROS level, since higher ROS production will result in CCO dysfunction (Srinivasan and Avadhani, 2012), indicating that fresh-cut melon had a lower ability to utilize O_2 during the oxidative phosphorylation process, leading to excessive $O_2^{\cdot -}$ accumulation. Both the TCA and CCP pathways are critical for energy provision of horticultural crops, since they generate large amounts of ATP. In this experiment, higher contents of ATP, ADP, NADH and NADPH and lower contents of NAD and NADP were detected in fresh-cut melon, which shows that cutting induced higher energy status, NADPH/NADP, and NADH/NAD. NAD(P) can receive electrons to form NAD(P)H in the respiratory electron-transport chain (RETC). The higher levels of NADPH/NADP and NADH/NAD in fresh-cut melon may lead to electron leakage from the RETC, thus producing large amounts of $O_2^{\cdot -}$. A higher energy status and an increased ROS level were found in fresh-cut melon, which agrees with a previous report where extracellular ATP accumulation triggered ROS production in injured fruit (Jacobo-Velázquez et al., 2011; Song et al., 2006). Although the content of ATP maintained a higher level in fresh-cut melon, only the activities of POD and GPX were enhanced at the early stage of storage, which is not consistent with the result of longan fruit treated with exogenous ATP (Lin et al., 2017). This different relationship between ATP and the antioxidant system activity may be attributed to species differences or storage conditions. Furthermore, these may indicate that the higher ATP content of fresh-cut melon resulted from the higher biochemical reactions involved in respiratory pathways and was not critical for the activation of the antioxidant system, while the ROS production was triggered. The energy released from the transformation of ATP to ADP based on H^+-ATPase and Ca^{2+}-ATPase is used for the physio-chemical metabolism, which could produce the beneficial substances that increase the resistance to cut-wounding stress (Jacobo-Velázquez et al., 2011). In this study, H^+-ATPase and Ca^{2+}-ATPase showed a similar changing pattern compared to ATP and ADP in fresh-cut melon. This also demonstrates that cutting increased the physio-chemical metabolism and large amounts of beneficial substances may be produced in fresh-cut melon, for example, phenolic accumulation (Jacobo-Velázquez et al., 2011) and wound suberization (Han et al., 2017). The results of qRT-PCR indicate the potential transcriptional level mechanism of ROS accumulation and energy metabolism in melon fruit in response to cut-wounding stress. These results were also found on the transcriptional level (except for SOD). In addition, the low commercial value was found in fresh-cut melon at the late stage of storage (data not shown), which may be related to the lower antioxidant system activity. These findings may give an insight into the relationship among the quality deterioration, ROS accumulation, and energy change in melon

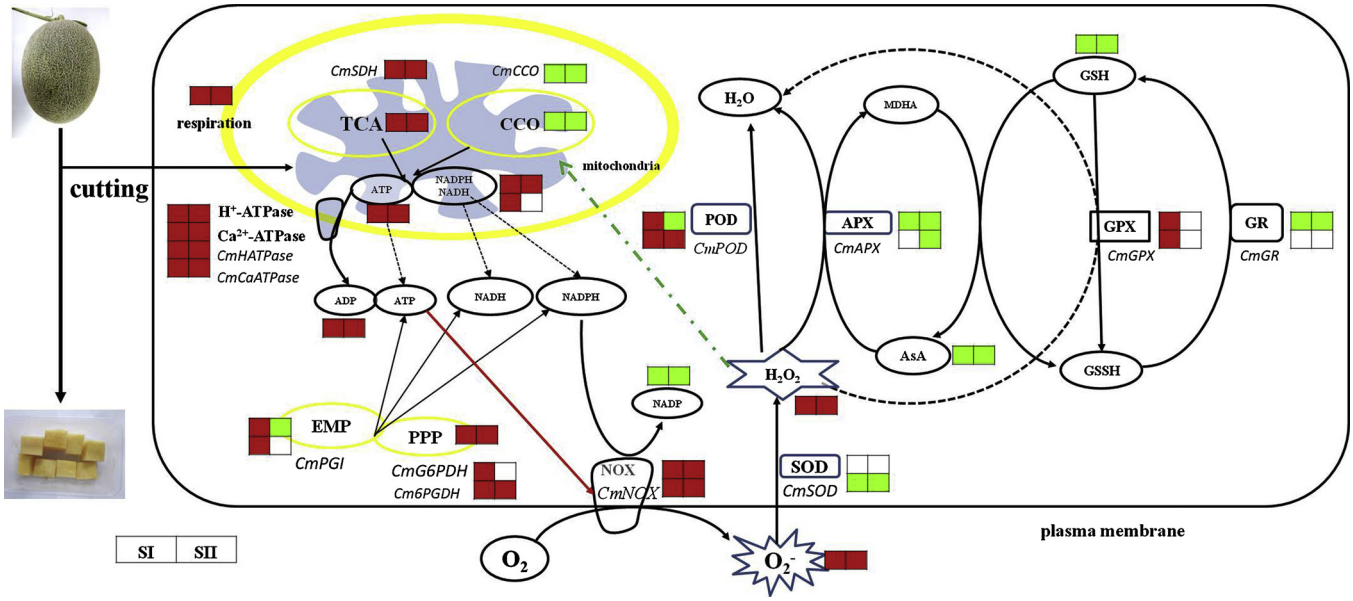

Fig. 7. A hypothetical model to explain the energy change affected by cutting in relation to ROS accumulation in melon fruit during storage at 15 °C. SI: early stage of storage of fresh-cut melon fruit; SII: late stage of storage of fresh-cut melon fruit. Red color means the significant up-regulation for metabolite content ($p < 0.05$), enzyme activity ($p < 0.05$) or gene expression (> 2.0-fold). Green color means the significant down-regulation for metabolite content ($p < 0.05$), enzyme activity ($p < 0.05$) or gene expression (< 0.5-fold). White color means no significant difference. All the significant differences are compared with whole fruit. (For interpretation of the references to colour in this figure legend, the reader is referred to the web version of this article).

during storage. Since ROS acts a signaling molecule for the wound-induced phenolic accumulation in fruits (Jacobo-Velázquez et al., 2011; Li et al., 2017b), these results will be very helpful to better study how to regulate ROS level to maximize the nutritional value of fresh-cut melon. However, further work is still required to understand the detailed mechanism of how ROS signal to resist the cut-wounding stress and how ATP is consumed in the biological metabolism of wounded fruit.

In summary, it is clear that cutting changed the respiratory metabolism pathway in melon during storage and also maintained higher activities of H^+-ATPase and Ca^{2+}-ATPase during storage. This led to large production of ATP, ADP, NADPH, and NADH in fresh-cut melon. Simultaneously, cutting enhanced the NOX activity, which resulted in a strong increase of ROS level in fresh-cut melon. Compared with whole fruit, both POD and GPX in fresh-cut melon were temporarily maintained at higher activities at the early stage of storage, while AsA, GSH, SOD, APX, and GR did not retain this higher level. Moreover, the lower antioxidant system activity in fresh-cut melon was found at the late stage of storage, which was indicated by lower contents of AsA and GSH and lower activities of POD, APX, and GR. These results indicate that melon changed its respiratory metabolism pathway in response to cut-wounding stress, which led to a higher energy status, accompanied by higher ROS accumulation. To explain the energy change affected by cutting in relation to ROS accumulation in melon, a hypothetical model was developed as shown in Fig. 7.

Declaration of Competing Interest

The authors have declared that no conflicts of interest exist.

Acknowledgment

This research was financially supported by the Innovation Project of Jiangsu Agricultural Science (CX (15) 1018).

Appendix A. Supplementary data

Supplementary material related to this article can be found, in the online version, at doi:https://doi.org/10.1016/j.scienta.2019.108752.

References

Acevedo, R.M., Maiale, S.J., Pessino, S.C., Bottini, R., Ruiz, O.A., Sansberro, P.A., 2013. A succinate dehydrogenase flavoprotein subunit-like transcript is upregulated in Ilex paraguariensis leaves in response to water deficit and abscisic acid. Plant Physiol. Biochem. 65, 48–54.

Aghdam, M.S., Jannatizadeh, A., Luo, Z., Paliyath, G., 2018. Ensuring sufficient intracellular ATP supplying and friendly extracellular ATP signaling attenuates stresses, delays senescence and maintains quality in horticultural crops during postharvest life. Trends Food Sci. Technol. 76, 67–81.

Amaro, A.L., Beaulieu, J.C., Grimm, C.C., Stein, R.E., Almeida, D.P.F., 2012. Effect of oxygen on aroma volatiles and quality of fresh-cut cantaloupe and honeydew melons. Food Chem. 130, 49–57.

Bradford, M.M., 1976. A rapid and sensitive method for the quantitation of microgram quantities of protein utilizing the principle of protein-dye binding. Anal. Biochem. 72, 248–254.

Chen, H., Han, S., Jiang, L., An, X., Yu, M., Xu, Y., Ma, R., Yu, Z., 2017. Postharvest hot air and hot water treatments affect the antioxidant system in peach fruit during refrigerated storage. Postharvest Biol. Technol. 126, 1–14.

Cocetta, G., Baldassarre, V., Spinardi, A., Ferrante, A., 2014. Effect of cutting on ascorbic acid oxidation and recycling in fresh-cut baby spinach (Spinacia oleracea L.) leaves. Postharvest Biol. Technol. 88, 8–16.

Errede, B., Kamen, M.D., Hatefi, Y., 1978. 8] Preparation and properties of complex IV (ferrocytochrome c: oxygen oxidoreductase EC 1.9.3.1). In: Fleischer, S., Packer, L. (Eds.), Methods in Enzymology. Academic Press, pp. 40–47.

Ge, Y., Deng, H., Bi, Y., Li, C., Liu, Y., Dong, B., 2015. Postharvest ASM dipping and DPI pre-treatment regulated reactive oxygen species metabolism in muskmelon (Cucumis melo L.) fruit. Postharvest Biol. Technol. 99, 160–167.

Gibon, Y., Larher, F., 1997. Cycling assay for nicotinamide adenine dinucleotides: NaCl precipitation and ethanol solubilization of the reduced tetrazolium⋆. Anal. Biochem. 251, 153–157.

Gil, M.I., Aguayo, E., Kader, A.A., 2006. Quality changes and nutrient retention in fresh-cut versus whole fruits during storage. J. Agric. Food Chem. 54, 4284–4296.

Guo, Q., Lv, X., Xu, F., Zhang, Y., Wang, J., Lin, H., Wu, B., 2013. Chlorine dioxide treatment decreases respiration and ethylene synthesis in fresh-cut 'Hami' melon fruit. Int. J. Food Sci. Technol. 48, 1775–1782.

Han, X., Lu, W., Wei, X., Li, L., Mao, L., Zhao, Y., 2017. Proteomics analysis to understand the ABA stimulation of wound suberization in kiwifruit. J. Proteomics 173, 42–51.

Hodges, D.M., Toivonen, P.M.A., 2008. Quality of fresh-cut fruits and vegetables as affected by exposure to abiotic stress. Postharvest Biol. Technol. 48, 155–162.

Huan, C., Jiang, L., An, X., Kang, R., Yu, M., Ma, R., Yu, Z., 2016. Potential role of glutathione peroxidase gene family in peach fruit ripening under combined postharvest treatment with heat and 1-MCP. Postharvest Biol. Technol. 111, 175–184.

Iakimova, E.T., Woltering, E.J., 2018. The wound response in fresh-cut lettuce involves programmed cell death events. Protoplasma 255, 1225–1238.

Jacobo-Velázquez, D.A., González-Agüero, M., Cisneros-Zevallos, L., 2015. Cross-talk between signaling pathways: the link between plant secondary metabolite production and wounding stress response. Sci. Rep. 5, 8608.

Jacobo-Velázquez, D.A., Martínez-Hernández, G.B., Rodríguez, S.D.C., Cao, C.M.,

Cisneros-Zevallos, L., 2011. Plants as biofactories: physiological role of reactive oxygen species on the accumulation of phenolic antioxidants in carrot tissue under wounding and hyperoxia stress. J. Agric. Food Chem. 59, 6583–6593.
Jiang, Y., Jiang, Y., Qu, H., Duan, X., Luo, Y., Jiang, W., 2007. Energy aspects in ripening and senescence of harvested horticultural crops. Stewart Postharvest Rev. 3, 1–5.
Li, L., Lv, F.Y., Guo, Y.Y., Wang, Z.Q., 2016. Respiratory pathway metabolism and energy metabolism associated with senescence in postharvest Broccoli (Brassica oleracea L. var. italica) florets in response to O 2 /CO 2 controlled atmospheres. Postharvest Biol. Technol. 111, 330–336.
Li, X., Li, M., Han, C., Jin, P., Zheng, Y., 2017a. Increased temperature elicits higher phenolic accumulation in fresh-cut pitaya fruit. Postharvest Biol. Technol. 129, 90–96.
Li, X., Li, M., Wang, J., Wang, L., Han, C., Jin, P., Zheng, Y., 2018. Methyl jasmonate enhances wound-induced phenolic accumulation in pitaya fruit by regulating sugar content and energy status. Postharvest Biol. Technol. 137, 106–112.
Li, X., Long, Q., Fan, G., Cong, H., Peng, J., Zheng, Y., 2017b. Effect of cutting styles on quality and antioxidant activity in fresh-cut pitaya fruit. Postharvest Biol. Technol. 124, 1–7.
Lin, Y., Chen, M., Lin, H., Hung, Y.C., Lin, Y., Chen, Y., Wang, H., Shi, J., 2017. DNP and ATP induced alteration in disease development of Phomopsis longanae Chi-inoculated longan fruit by acting on energy status and reactive oxygen species production-scavenging system. Food Chem. 228, 497–505.
Luo, H., Li, Z., Jiang, J., Yu, Z., 2012. Quality changes of whole and fresh-cut Zizania latifolia during refrigerated (1 °C) storage. Food Bioprocess. Technol. 5, 1411–1415.
Ortiz-Duarte, G., Pérez-Cabrera, L.E., Artés-Hernández, F., Martínez-Hernández, G.B., 2019. Ag-chitosan nanocomposites in edible coatings affect the quality of fresh-cut melon. Postharvest Biol. Technol. 147, 174–184.
Palma, F., Carvajal, F., Ramos, J.M., Jamilena, M., Garrido, D., 2015. Effect of putrescine application on maintenance of zucchini fruit quality during cold storage: contribution of GABA shunt and other related nitrogen metabolites. Postharvest Biol. Technol. 99, 131–140.
Reyes, L.F., Villarreal, J.E., Cisneros-Zevallos, L., 2007. The increase in antioxidant capacity after wounding depends on the type of fruit or vegetable tissue. Food Chem. 101, 1254–1262.
Sagi, M., Fluhr, R., 2001. Superoxide production by plant homologues of the gp91(phox) NADPH oxidase. Modulation of activity by calcium and by tobacco mosaic virus infection. Plant Physiol. 126, 1281–1290.
Sharom, M., Willemot, C., Thompson, J.E., 1994. Chilling injury induces lipid phase changes in membranes of tomato fruit. Plant Physiol. 105, 305.
Shetty, N.P., Jørgensen, H.J.L., Jensen, J.D., Collinge, D.B., Shetty, H.S., 2008. Roles of reactive oxygen species in interactions between plants and pathogens. Eur. J. Plant Pathol. 121, 267–280.
Ślaski, J.J., Zhang, G., Basu, U., Stephens, J.L., Taylor, G.J., 1996. Aluminum resistance in wheat (Triticum aestivum) is associated with rapid, Al-induced changes in activities of glucose-6-phosphate dehydrogenase and 6-phosphogluconate dehydrogenase in root apices. Physiol. Plant. 98, 477–484.
Soliva-Fortuny, R.C., Martín-Belloso, O., 2003. New advances in extending the shelf-life of fresh-cut fruits: a review. Trends Food Sci. Technol. 14, 341–353.
Song, C.J., Iris, S., Xuanzhi, W., Stout, S.C., Roux, S.J., 2006. Extracellular ATP induces the accumulation of superoxide via NADPH oxidases in Arabidopsis. Plant Physiol. 140, 1222.
Srinivasan, S., Avadhani, N.G., 2012. Cytochrome c oxidase dysfunction in oxidative stress. Free Radic. Biol. Med. 53, 1252–1263.
Wang, J., Mao, L., Li, X., Lv, Z., Liu, C., Huang, Y., Li, D., 2018. Oxalic acid pretreatment reduces chilling injury in Hami melons (Cucumis melo var. reticulatus Naud.) by regulating enzymes involved in antioxidative pathways. Sci. Hortic. 241, 201–208.
Wang, Y., Luo, Z., Khan, Z.U., Mao, L., Ying, T., 2015. Effect of nitric oxide on energy metabolism in postharvest banana fruit in response to chilling stress. Postharvest Biol. Technol. 108, 21–27.
Xu, G., Liu, D., Chen, J., Ye, X., Ma, Y., Shi, J., 2008. Juice components and antioxidant capacity of citrus varieties cultivated in China. Food Chem. 106, 545–551.